Contrariety and inhibition enhance synchronization in a small-world network of phase oscillators

Tayebe Nikfard, Yahya Hematyar Tabatabaei, and Farhad Shahbazi *
Department of Physics, Isfahan University of Technology, Isfahan 84156-83111, Iran

(Received 10 November 2020; revised 27 September 2021; accepted 11 November 2021; published 24 November 2021)

We numerically study Kuramoto model synchronization consisting of the two groups of conformist-contrarian and excitatory-inhibitory phase oscillators with equal intrinsic frequency. We consider random and small-world (SW) topologies for the connectivity network of the oscillators. In random networks, regardless of the contrarian to conformist connection strength ratio, we found a crossover from the π-state to the blurred π-state and then a continuous transition to the incoherent state by increasing the fraction of contrarians. However, for the excitatory-inhibitory model in a random network, we found that for all the values of the fraction of inhibitors, the two groups remain in phase and the transition point of fully synchronized to an incoherent state reduced by strengthening the ratio of inhibitory to excitatory links. In the SW networks we found that the order parameters for both models do not show monotonic behavior in terms of the fraction of contrarians and inhibitors. Up to the optimal fraction of contrarians and inhibitors, the synchronization rises by introducing the number of contrarians and inhibitors and then falls. We discuss that the nonmonotonic behavior in synchronization is due to the weakening of the defects already formed in the pure conformist and excitatory agent model in SW networks. We found that in SW networks, the optimal fraction of contrarians and inhibitors remain unchanged for the rewiring probabilities up to ~ 0.15, above which synchronization falls monotonically, like the random network. We also showed that in the conformist-contrarian model, the optimal fraction of contrarians is independent of the strength of contrarian links. However, in the excitatory-inhibitory model, the optimal fraction of inhibitors is approximately proportional to the inverse of inhibition strength.

DOI: 10.1103/PhysRevE.104.054213

I. INTRODUCTION

The Kuramoto model originally introduced by Kuramoto [1,2] is a simple and mathematically tractable model showing the synchronization transition in an ensemble of mutually interacting phase oscillators (rotors). Synchronization is ubiquitous, such as flashing of fireflies, flocking of birds and fishes, the simultaneous firing of brain neurons, and heart cells [3–7].

While Kuramoto's motivation for introducing his model was to find an exactly solvable model for the transition from desynchronized to synchronized states, this model found many applications in physical, chemical, and biological systems [8]. The Kuramoto model and its variants have been used to model the opinion formation dynamics in a society [9–13]. In this context, the phase of each individual corresponds to its belief, and synchronization is equivalent to the formation of consensus in society.

In the original Kuramoto model, the rotors globally coupled to each other sinusoidally with uniform coupling constant. The exact solution of this model indicates a continuous synchronization at a critical coupling [8]. Recent developments in complex network science attracted the researchers to the study of synchronization in general [14] and the Kuramoto model with local interactions in complex networks [15]. For instance, the Kuramoto model has been studied on the regular [16,17] and small-world SW networks [18–23]. In this regard, some impressive results are forming patterns of synchrony in regular and Watts-Strogatz networks for a group of identical phase oscillators. In a regular ring shape network, the patterns are helical, topologically distinct, and characterized by integer winding numbers [16,17]. Rewiring the ring's links with a small probability between 0.005 and 0.05 converts the regular lattice to the SW network, which has the small-world properties of small mean shortest path and high clustering [19,24]. This process turns the helical patterns into several isolated defects or deviated helical patterns for small and large winding numbers, respectively [23]. In isolated defects, the phase difference between their center and surroundings varies continuously from 0 to π by going away from the center.

Esfahani *et al.* found that adding a spatially uncorrelated white noise to the Kuramoto model could destroy theses defects and make a more homogenous phase texture with higher phase-synchrony, that is, *stochastic synchronization* [23]. Moreover, they showed that the significant rewiring probabilities larger than 0.15 destroy the defects and so set the system in a full synchronization state [23].

To make the Kuramoto model closer to reality, the generalization of the model with random pairwise coupling with both signs was investigated [25–27]. While the positive coupling encourages that the phases of interacting oscillators converge to an in-phase state, the negative coupling forces them to align in an antiphase (π-difference) configuration. Initially, a glassy behavior was claimed for this model [25]; however, later investigations shed doubt on the existence and properties of such a state [26,27].

*shahbazi@iut.ac.ir

Hong and Strogatz introduced a simpler version of the model with mixed coupling in which the oscillators are divided into two groups of conformists and contrarians [12,13]. In this model the conformists have positive coupling with the rest of oscillators and so tend to be in line with the dominant rhythm of the population; however, the contrarians have negative coupling with the rest and are prone to move in the opposite direction of population. Hong and Strogatz investigated the model both with [12] and without [13] intrinsic angular-velocity distribution and found a rich phase diagram for this model in terms of the fraction of conformists. The phase diagram includes the desynchronized, antiphase locked state between the conformists and contrarians, and the traveling waves in which the average angular velocity is different from the mean intrinsic angular-velocity distribution. Surprisingly, they found that the identical phase-oscillator model has a richer phase diagram.

Motivated by Hong and Strogatz, in this work we study the Kuramoto model of two groups of conformist and contrarian phase oscillators, which are identical in terms of their intrinsic angular velocities, in a SW network. Moreover, we also investigate a Kuramoto model of excitatory and inhibitor phase oscillators in the SW network, in which a given rotor is coupled positively to its excitatory and negatively to its inhibitor neighbors.

The paper is organized as follows: In Sec. II we define the model and the numerical methods of quantifying the synchronization. Section III represents the results and discussion, and section IV is devoted to the concluding remarks.

II. MODEL AND METHOD

In this work we study two Kuramoto models in bidirected random and Watts-Strogatz small-world networks. The two models are (i) the conformist-contrarian model and (ii) the excitatory-inhibitory model. Each model consists of N phase oscillators (rotors) divided into two groups (conformist-contrarian and excitatory-inhibitory). The rotors occupy the vertices of a network, and each interacts with its neighbors through a sinusoidal coupling whose argument is their phase difference. However, the coupling is not symmetric.

A. Conformist-contrarian model

The conformist-contrarian model is given by a set of coupled first-order differential equations as

$$\frac{d\theta_i^s}{dt} = \omega_0 + \frac{\lambda_i^s}{k_i}\sum_{j=1}^{N} a_{ij}\sin\left(\theta_j - \theta_i^s\right), \quad i = 1, ..., N, \tag{1}$$

where θ_i denotes the phase of the oscillator sitting at node i, and ω_0 is the intrinsic frequency of the oscillators and is considered equal for all of them. a_{ij} denotes the elements of the adjacency matrix of a bidirected network (i.e., $a_{ij} = a_{ji} = 1$ if i and j are connected and $a_{ij} = 0$ otherwise), and k_i is the degree of node i. λ^s, where $s =$ conformist, contrarian), is the coupling constant, which is positive for the conformist and negative for the contrarians. Indeed, a conformist with positive coupling inclines to align its phase with its neighbors' phases, while a contrarian tries to direct its phase as far as possible to its neighbors.

The intrinsic frequency, ω_0, can always be set to zero by moving to a rotating frame with the angular velocity ω_0, i.e., $\theta'(t) = \theta(t) - \omega_0 t$. Moreover, by defining the dimensionless time $\tau = \lambda^{\text{conf}} t$, Eq. (1) converts to

$$\frac{d\theta'^{\text{conf}}_i}{d\tau} = \frac{1}{k_i}\sum_{j=1}^{N} a_{ij}\sin\left(\theta'_j - \theta'^{\text{conf}}_i\right),$$

$$\frac{d\theta'^{\text{cont}}_i}{d\tau} = -\frac{Q}{k_i}\sum_{j=1}^{N} a_{ij}\sin\left(\theta'_j - \theta'^{\text{cont}}_i\right), \tag{2}$$

where we assumed $\lambda^{\text{cont}} = -Q\lambda^{\text{conf}}$, with $Q > 0$ and $\lambda^{\text{conf}} > 0$ (cont and conf stand for contrarian and conformist, respectively).

B. Excitatory-inhibitory model

Now consider a system consisting of two groups of excitatory and inhibitory phase oscillators. Each oscillator receives a positive input from its excitatory and negative input from its inhibitory neighbors in this system. Therefore the coupling λ_j^s has to inserted inside the sum, and then we find

$$\frac{d\theta_i}{dt} = \omega_0 + \frac{1}{k_i}\sum_{j=1}^{N} a_{ij}\lambda_j^s\sin\left(\theta_j^s - \theta_i\right), \quad i = 1, ..., N, \tag{3}$$

in which we assume $\lambda_i^{\text{inhib}} = -Q\lambda_i^{\text{excit}}$ with $Q > 0$ and $\lambda^{\text{excit}} > 0$ (inhib and excit stand for inhibitory and excitatory, respectively). Similarly, after moving to the rotating frame with angular velocity ω_0 and rescaling the time variable as $\tau = \lambda^{\text{excit}} t$, we get

$$\frac{d\theta'_i}{d\tau} = \frac{1}{k_i}\sum_{j\in\text{excit}} a_{ij}\sin(\theta'_j - \theta'_i) - \frac{Q}{k_i}\sum_{j\in\text{inhib}} a_{ij}\sin(\theta'_j - \theta'_i). \tag{4}$$

C. Method

To obtain the time evolution of the phase of the oscillators, we use the fourth-order Runge-Kutta method for integrating the sets of equations (2) and (4). The initial phase distribution is taken from a box distribution in the interval $[-\pi, \pi]$, and the integration time step is set to $d\tau = 0.1$. To make sure that the integration time step 0.1 is a good choice, we used the smaller time step 0.01 for some simulations and found that the results remain unchanged for both integration time steps.

The global synchrony among the oscillators at any time can be measured by the Kuramoto order parameter, defined as

$$\mathbf{r}(\tau) = \frac{1}{N}\sum_{j=1}^{N}\exp\left(i\theta_j(\tau)\right). \tag{5}$$

In the stationary state we define the long time averaged order parameter as r_∞:

$$\mathbf{r}_\infty = \lim_{\Delta\tau\to\infty}\frac{1}{\Delta\tau}\int_{\tau_s}^{\tau_s+\Delta\tau} r(\tau)d\tau, \tag{6}$$

in which τ_s is the time of reaching a stationary state. The magnitude of $\mathbf{r}_\infty$ shown by r_∞ is a real number between

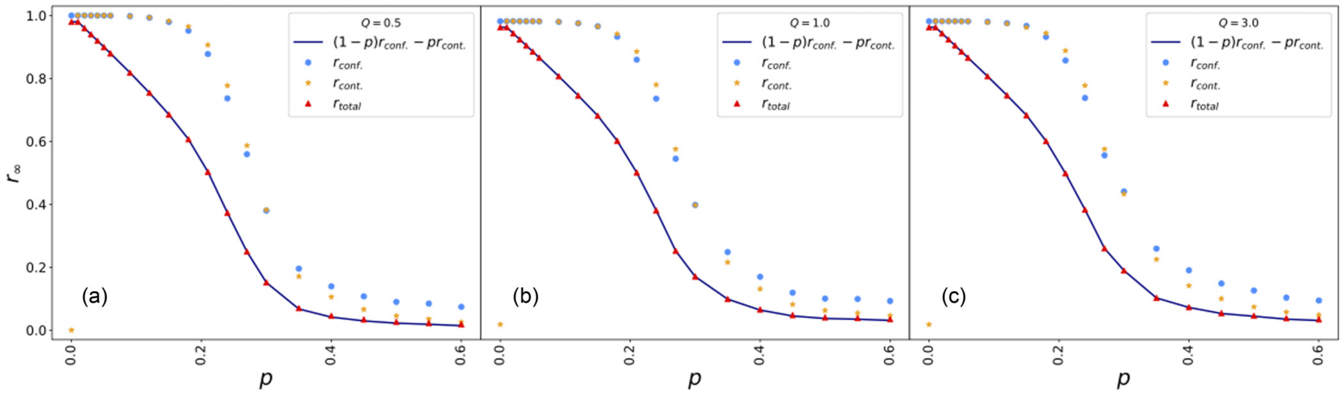

FIG. 1. Stationary total and partial order parameters vs fraction of contrarians for the conformist-contrarian model [Eq. (2)] for (a) $Q = 0.5$, (b) $Q = 1.0$, and (c) $Q = 3.0$ for a random network of $N = 1000$ oscillators and mean degree $< k >= 10$.

0 and 1. $r_\infty = 0$ indicates a disordered or a phase-locked state with regular phase lag, $0 < r_\infty < 1$ indicates a partially synchronized state, and $r_\infty = 1$ shows the full synchrony in the system.

We also define a partial order parameter for the two groups of oscillators as

$$\mathbf{r}_a(\tau) = r_a(\tau)\exp(i\Theta_a(\tau)) = \frac{1}{N_a}\sum_{j\in a}\exp(i\theta_j^a(\tau))\cdot \ a = 1, 2, \tag{7}$$

where $a = 1$ refers to conformist and excitatory and $a = 2$ to contrarian and inhibitory oscillators. r_a and Θ_a are the magnitude and phase of the partial order parameter. For each model the fraction of contrarian ($\frac{N_{ct}}{N}$) and inhibitory ($\frac{N_{in}}{N}$) oscillators is denoted by p.

It can be easily seen that Eqs. (5) and (7) give rise to

$$\mathbf{r}(\tau) = (1 - p)\mathbf{r}_1(\tau) + p\mathbf{r}_2(\tau), \tag{8}$$

from which one found the following expression for the magnitude of the total order parameter in terms of the magnitude of partial order parameters and their phase difference:

$$r = \sqrt{(1 - p)^2 r_1^2 + p^2 r_2^2 + 2p(1 - p)r_1 r_2 \cos(\Theta_1 - \Theta_2)}. \tag{9}$$

The Kuramoto order parameter is a measure of global synchronization in the system. To gain insight into the local coherence in the stationary state, we calculate the pairwise correlation matrix D [28]:

$$D_{ij} = \lim_{\Delta\tau\to\infty} \frac{1}{\Delta\tau}\int_{\tau_s}^{\tau_s+\Delta\tau} \cos(\theta_i(\tau) - \theta_j(\tau))d t. \tag{10}$$

The matrix elements D_{ij} take a value in the interval $[-1, 1]$. $D_{ij} = 1$ denotes full synchrony between oscillators i and j, while $D_{ij} = -1$ represents an antiphase state (i.e., $|\theta_i - \theta_j| = \pi$).

The phase diagram of the conformist-contrarian model, with identical intrinsic frequency, has been obtained by Hong and Strogatz [13]. This phase diagram includes four phases:

(a) An *incoherent* phase where both partial order parameters are zero ($r_1 = r_2 = 0$);

(b) A *blurred* π-state, where the conformists and contrarians are partially ordered ($r_1, r_2 < 1$) but there is π difference between the phase of their order parameters $|\Theta_1 - \Theta_2| = \pi$, and the incoherent and blurred π-states coexists together for some range of fraction of contrarians;

(c) A *traveling wave* state, where the conformist are completely ordered $r_1 = 1$, but the contrarians are partially

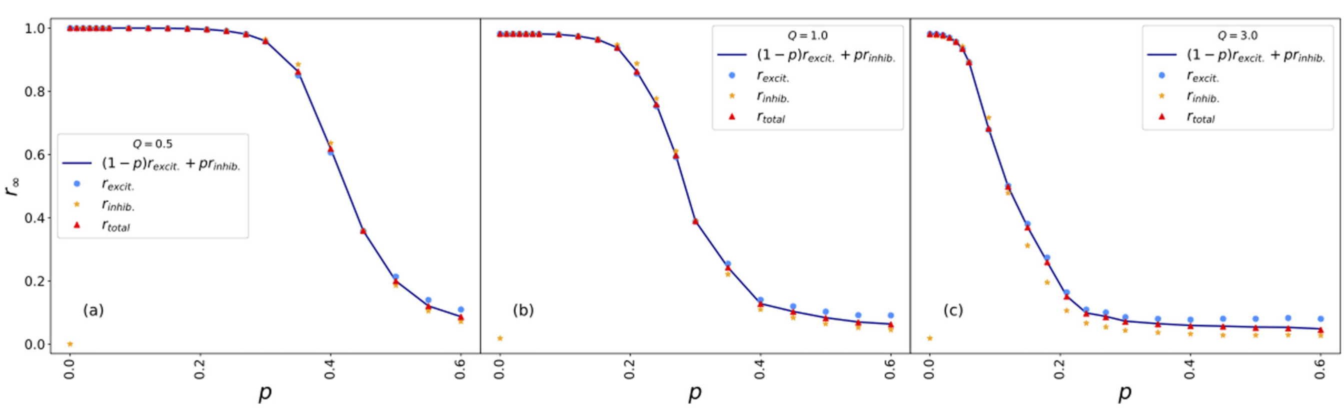

FIG. 2. Stationary total and partial order parameters vs fraction of inhibitory oscillators for the excitatory-inhibitory [Eq. (4)] model for (a) $Q = 0.5$, (b) $Q = 1.0$, and (c) $Q = 3.0$ for a random network of $N = 1000$ oscillators and mean degree $< k >= 10$.

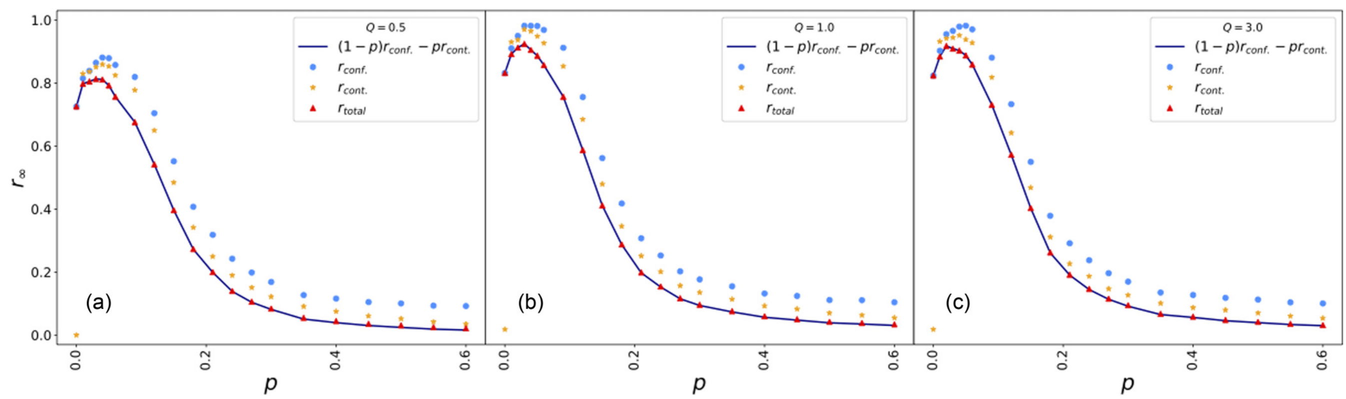

FIG. 3. Stationary total and partial order parameters vs fraction of contrarians for the conformist-contrarian model [Eq. (2)] for (a) $Q = 0.5$, (b) $Q = 1.0$, and (c) $Q = 3.0$ for a SW network of $N = 1000$ oscillators and mean degree $< k >= 10$.

ordered $r_2 < 1$, and in this case, the absolute phase difference of these order parameters could be less than π, and

(d) The π-state, where both conformists and contrarians are fully synchronized $r_1 = r_2 = 1$ and their phase difference is equal to π ($|\Theta_1 - \Theta_2| = \pi$).

In the next section we proceed to investigate the phase diagram of both conformist-contrarian and excitatory-inhibitory models in random and small-world networks. The networks used in this study are created by the Watts-Strogatz algorithm [19,24]. To build an SW network, starting from a ring with a given degree of k for each node, we rewire the links with the probability 0.03, and for the random network, we rewire them with probability 1.

III. RESULTS AND DISCUSSION

Since we did not find remarkable size dependence for the networks larger than $N = 200$, we performed all the simulations on the size $N = 1000$. Moreover, since we are interested in applying the models in real networks that are mostly sparse, we consider the mean degree of 10. We check that, as far as the network is sparse, the results remain unchanged. In the following we report the results of both models in random and then in small-world networks.

A. Random network

In random networks for the conformist-contrarian model, the simulations typically reach the stationary state up to ∼10 000 time steps. Figure 1 represents the variation of the magnitude of long-time averaged total (r_∞) and partial order parameters ($r_{\rm conf}$ and $r_{\rm cont}$) vs the fraction of contrarians (p) for the conformist-contrarian model with $Q = 0.5, 1.0, 3.0$. Each data is obtained by averaging over 100 independent distribution of contrarians.

Our calculations indicate that for all ranges of p, the phase difference between two partial order parameters is equal to π, i.e., the system is in π or blurred π-state for all values of p. In this case, Eq. (9) results in the following relation for the stationary total order parameter in terms of the partial order parameters:

$$r_\infty = (1-p)r_{\rm conf} - pr_{\rm cont}. \tag{11}$$

The solid line in Fig. 1 is the plot of Eq. (11) which completely lies on the total order parameter data. This figure shows, regardless of the value of Q, the magnitude of partial order parameters is near unity for $p \lesssim 0.12$, giving rise to a linear dependence of r_∞ vs p with the slope -2 in this range of p. It means that the stable state of the system in this region is the π-state. However, for $p > 0.12$, conformists and contrarians' partial order parameters are less than unity, indicating that

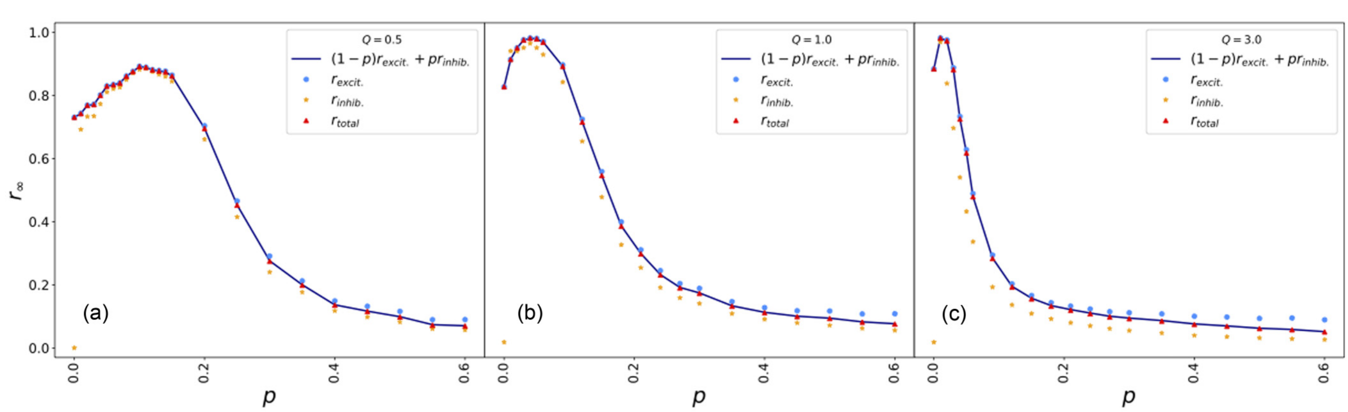

FIG. 4. Stationary total and partial order parameters vs fraction of inhibitory oscillators for the excitatory-inhibitory [Eq. (4)] model for (a) $Q = 0.5$, (b) $Q = 1.0$, and (c) $Q = 3.0$ for a SW network of $N = 1000$ oscillators and mean degree $< k >= 10$.

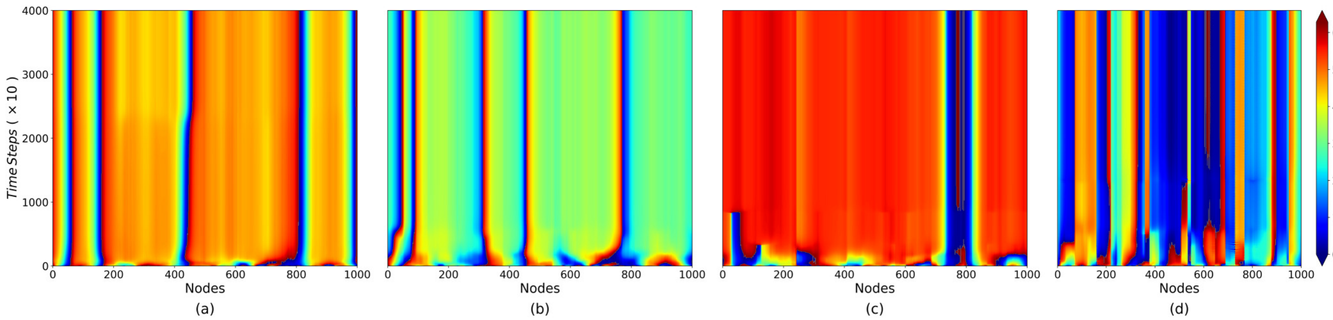

FIG. 5. Temporal evolution of the phases of rotors in a single realization of the conformist-contrarian model [Eq. (2)], with $Q = 1.0$, in an SW network for (a) $p = 0.0$, (b) $p = 0.03$, (c) $p = 0.05$, and (d) $p = 0.09$.

they have more freedom to swing their phase; then the system is the blurred π-state. Our results denote that the traveling wave states are not present in a random network with sparse connectivity, unlike the all-to-all network.

The variation of the order parameters in terms of the fraction of contrarians does not depend on Q. Such independence, if the stationary results to the parameter Q, can be easily justified by absorbing Q into the dimensionless time parameter τ in Eq. (2), which drops Q from the right-hand side of this equation. It means that Q only affects the contrarians' stationary timecale; hence, the results in the stationary state do not depend on Q.

Indeed, we find a crossover from the π-state to the blurred π-state at the same p for all values of Q. This result is in sharp contrast with the complete network. A traveling wave (TW) state mediates the π-state and blurred π-state. The transition between the π-state and TW is discontinuous, while TW continuously connects to the blurred π-state [13].

The stationary time for the excitatory-inhibitory model is more considerable and could be up to ~35 000 time steps. Figure 2 displays the dependence of the magnitude of stationary total order parameter (r_∞) and partial order parameters ($r_{\rm excit}$ and $r_{\rm inhib}$) to the fraction of inhibitory oscillators (p) for the model with $Q = 0.5, 1.0, 3.0$. Each data is obtained by averaging over 100 independent distribution of inhibitors.

We found that the excitatory and inhibitory oscillators have the same phase for all p and Q for this model, which can be verified by the exact overlap of the equation

$$r_\infty = (1 - p)r_{\rm excit} + pr_{\rm inhib}, \qquad (12)$$

with the total order parameter, illustrated in Fig. 2.

Interestingly, the system remains in a fully synchronized state (up to $p \sim 0.3$) for $Q = 0.5$, and the range of full synchrony decreases by increasing Q. Indeed, at small enough p, the minority inhibitors synchronize with each other through their neighboring majority excitatory oscillators. The larger Q also reduces the transition point to the incoherent state. This result is not surprising; as expected, the strengthening of the inhibitory links leads to the faster vanishing of the synchronized state.

B. Small-world network

The time to reach a stationary state in an SW network (Watts-Strogatz network with rewiring probability 0.03) is an order of magnitude larger than those of random networks for both models and could as large as 6×10^5 time steps.

Figures 3 and 4 illustrate the variations of the total and partial order parameters in terms of the fraction of contrarian and inhibitors for the conformist-contrarian and excitatory-inhibitory models, respectively. For both models we adapt $Q = 0.5, 1.0, 3.0$, and each data point is obtained by averaging over independent random initial conditions. In contrast to the random network, the averaged order parameters are less than unity for $p = 0$, which is due to the formation of the defect patterns in small-world networks [23]. Indeed, for a group of identical phase oscillators, depending on the initial phase distribution, the magnitude of stationary order parameters varies between 0 and 1; then its average is less than 1. The oscillators in the center of defects are in a π-locked state with those in the homogeneous parts, indicating that the Kuramoto

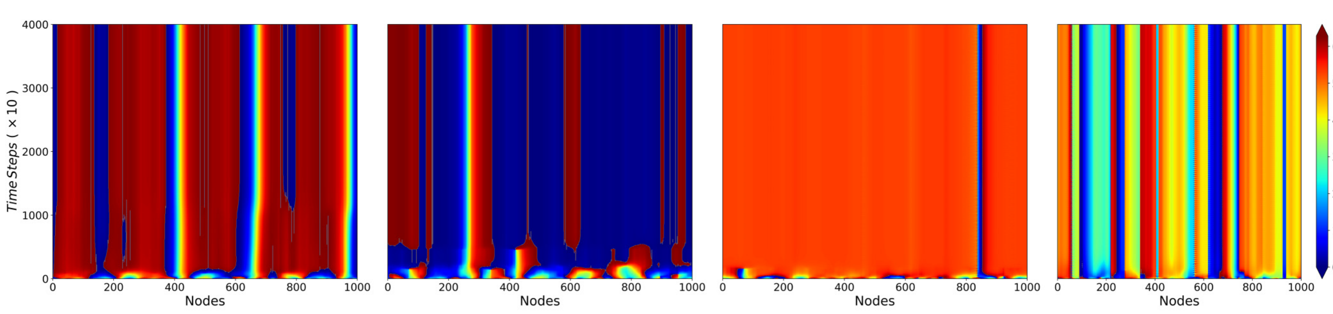

FIG. 6. Temporal evolution of the phases of rotors in a single realization of the excitatory-inhibitory model [Eq. (4)], with $Q = 1.0$, in an SW network for (a) $p = 0.0$, (b) $p = 0.03$, (c) $p = 0.05$, and (d) $p = 0.09$.

dynamics turns some individual oscillators to contrarians even for an identical ensemble of phase oscillators.

Figure 3 shows that the behavior of order parameters versus the fraction of contrarians does not depend on Q, and like the random network, the exact overlap of the total order parameter and the relation $r_\infty = (1 - p)r_{\rm conf} - pr_{\rm cont}$ indicates that the phase difference between conformist and contrarians are always equal to π. Hence the system is in a blurred π-state for all values of p and Q. Moreover, Fig. 3 represents the enhancement of synchronization by increasing the fraction of contrarians to $p \sim 0.04$, at which the synchrony reaches a maximum and then begins to fall by further increase of p.

For the excitatory-inhibitory model, as can be seen in Fig. 4, the relation $r_\infty = (1 - p)r_{\rm excit} + pr_{\rm inhib}$ fits very well with the total order parameter, meaning that the excitatory and inhibitory oscillators, regardless of the value of p and Q, are always in-phase. This model also shows a maximum for the total order parameter; however, the optimal value of p, which leads to this maximum synchrony, decreases by increasing the strength of inhibitory links to the excitatory ones.

The nonmonotonic behavior of order parameters versus p can be explained by weakening and reducing the defects as the contrarians or inhibitors are introduced to the dynamics. Figures 5 and 6 respectively represent the evolution of the phases of the rotors for a single realization of the conformist-contrarian and excitatory-inhibitory models with $Q = 1$. Both figures show the remarkable reduction of the isolated defects in going from $p = 0.03$ to 0.05.

To make sure that theses results are not the artifact of using only a fixed network realization, we performed the above simulations on ten realizations of SW network with the same number of nodes, degree, and rewiring probability but with different adjacency matrices and observed similar results in all of them. As a result, when several contrarians and inhibitors are randomly substituted in the network, some sit in the vicinity of defect locations. The perturbing effect of these new agents on the oscillators inside the defects, which are in an antiphase state with other oscillators of their group, give them more freedom to deviate from their previous antiphase state and so lead to the weakening of the defects. When the fraction of contrarians or inhibitors reaches an optimal value, they give maximal freedom to the defects and lift the synchronization to a maximum. As explained before, the optimal value of p is independent of Q for the conformist-contrarian model; however, in the excitatory-inhibitory model, increasing the inhibitory links' weight gives rise to a more substantial perturbation and therefore tends to decrease the optimal p.

To wrap up this section, we investigate the effect of rewiring probability and the strength of contrariety or inhibition in the above results. As discussed before, for the conformist-contrarian model the contrariety strength Q does not have any effect on the stationary features of the model and so the optimal fraction of contrarians is independent of Q. Nevertheless, in the excitatory-inhibitory model the optimal fraction of inhibitors p_m, at which the synchrony reaches a maximum, decreases by increasing the strength of the inhibitors Q. Figure 7 illustrates the dependence of p_m on Q for a SW network with rewiring probability 0.03. This figure displays a power law relation between p_m and Q with an exponent close to -1, implying that the effect of inhibitors in the collective behavior of system is approximately proportional to Q.

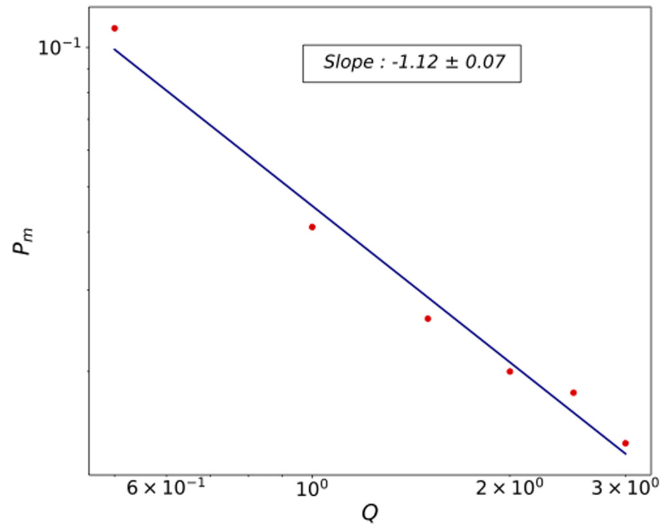

FIG. 7. Log-log plot of optimal fraction of inhibitory oscillators (p_m) vs their link strength Q in a small-world network of excitatory-inhibitory rotors of size $N = 1000$ and mean degree $< k >= 10$ and with rewiring probabilities $p = 0.03$.

In terms of the probability rewiring p_r, we found that for both models the optimal fraction of contrarians or inhibitors is nearly independent of the rewiring probability up to $p_r \sim 0.15$, above which the peak in synchrony vanishes and the system behaves like a random network. (See Fig. 8 for the conformist-contrarian model.)

IV. CONCLUSION

In summary, we numerically investigated the Kuramoto model with two groups of conformist-contrarian and

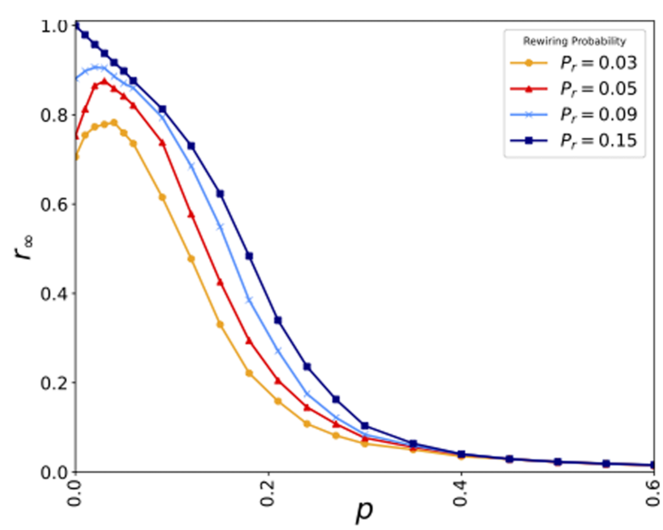

FIG. 8. Stationary order parameters vs fraction of contrarians for the conformist-contrarian model [Eq. (2)] for $Q = 1$ and in a small-world of $N = 1000$ oscillators and mean degree $< k >= 10$ with rewiring probabilities $p_r = 0.03, 0.05, 0.09, 0.15$.

excitatory-inhibitory phase oscillators, with the same intrinsic frequency, in the sparse random and Watts-Strogatz SW networks. In random networks, the conformist-contrarian model finds a stationary state with a π-state that crosses over to a blurred π-state by increasing the fraction of contrarians. On the other hand, for the SW network the system is always in a blurred π-state where both conformists and contrarians are partially synchronized, and unlike the all-to-all network, the traveling wave state does not appear in both networks. For the excitatory-inhibitory model, we found that both types of oscillators are always in-phase in random and SW networks.

Interestingly, for both models in SW networks, we observed nonmonotonic variation of the stationary order parameter versus the fraction of contrarians and inhibitors; the synchronization first increases and reaches a maximum at an optimal fraction of contrarians or inhibitors. Indeed, one expects that the impurities like contrarians or inhibitors have destructive roles in the population synchrony. Therefore, increasing the synchrony up an optimal value of a fraction of contrarians and inhibitors seems counterintuitive.

We explained that the above results are due to the attenuation of preexisting defects of the SW network when the contrarians or inhibitors are added to the system. We note that enhancement of synchronization by contrariety and inhibition in this model could be considered an implication of *asymmetry-induced symmetry* [29–32], stating that a more symmetric state can be induced in an oscillator system by reducing the symmetry of pairwise interactions. Here we found that the symmetry reduction in the couplings of a group of interacting identical oscillators in an SW network pushes it to a more symmetric state by elevating the system's level of synchrony.

For the conformist-contrarian model, the optimal fraction of contrarians at which the order parameter reaches a peak is independent of contrariety strength. However, for the excitatory-inhibitory model, the optimal fraction of inhibitors is approximately proportional to the inverse of the inhibition strength. However, we found that for a given value of contrariety or inhibition strength, the optimal values of contrarians or inhibitors hardly depend on the rewiring probability of the SW network, and for the rewiring probabilities larger than ~ 0.15, both models show behaviors similar to the random network.

We hope that this work gains more insight into the constructive role of diversity, appearing in the form of contrarians in human societies and inhibitors in neuronal networks which are known to have small-world connectivity.

ACKNOWLEDGMENTS

The authors gratefully acknowledge the Sheikh Bahaei National High-Performance Computing Center (SBNHPCC) for providing computing facilities and time. SBNHPCC is supported by the Scientific and Technological Department of the presidential office and Isfahan University of Technology (IUT).The authors declare that they have no conflict of interest.

[1] Y. Kuramoto, in *International Symposium on Mathematical Problems in Theoretical Physics* (Springer, New York, 1975), pp. 420–422.
[2] Y. Kuramoto, *Chemical Oscillations, Waves, and Turbulence*, Vol. 19 (Springer Science & Business Media, New York, 2012), Vol. 19.
[3] A. T. Winfree, *The Geometry of Biological Time*, Vol. 12 (Springer Science & Business Media, New York, 2001), Vol. 12.
[4] A. Pikovsky, M. Rosenblum, and J. Kurths, *Synchronization: A Universal Concept in Nonlinear Sciences* (Cambridge University Press, Cambridge, England, 2003), Vol. 12.
[5] S. C. Manrubia, A. S. Mikhailov *et al.*, *Emergence of Dynamical Order: Synchronization Phenomena in Complex Systems* (World Scientific, Singapore, 2004), Vol. 2.
[6] A. Balanov, N. Janson, D. Postnov, and O. Sosnovtseva, *Synchronization: From Simple to Complex* (Springer Science & Business Media, New York, 2008).
[7] S. Strogatz, *Sync: How Order Emerges from Chaos in the Universe, Nature, and Daily Life* (Hachette Books, New York, 2012).
[8] J. A. Acebrón, L. L. Bonilla, C. J. P. Vicente, F. Ritort, and R. Spigler, Rev. Mod. Phys. **77**, 137 (2005).
[9] A. Pluchino, V. Latora, and A. Rapisarda, Int. J. Mod. Phys. C **16**, 515 (2005).
[10] A. Pluchino, V. Latora, and A. Rapisarda, Eur. Phys. J. B **50**, 169 (2006).
[11] A. Pluchino, S. Boccaletti, V. Latora, and A. Rapisarda, Physica A **372**, 316 (2006).
[12] H. Hong and S. H. Strogatz, Phys. Rev. E **84**, 046202 (2011).
[13] H. Hong and S. H. Strogatz, Phys. Rev. Lett. **106**, 054102 (2011).
[14] A. Arenas, A. Díaz-Guilera, J. Kurths, Y. Moreno, and C. Zhou, Phys. Rep. **469**, 93 (2008).
[15] F. A. Rodrigues, T. K. D. Peron, P. Ji, and J. Kurths, Phys. Rep. **610**, 1 (2016).
[16] D. A. Wiley, S. H. Strogatz, and M. Girvan, Chaos **16**, 015103 (2006).
[17] R. Delabays, M. Tyloo, and P. Jacquod, Chaos **27**, 103109 (2017).
[18] P. M. Gade and C.-K. Hu, Phys. Rev. E **62**, 6409 (2000).
[19] D. J. Watts, *Small Worlds: The Dynamics of Networks between Order and Randomness* (Princeton University Press, Princeton, NJ, 2001).
[20] H. Hong, M.-Y. Choi, and B. J. Kim, Phys. Rev. E **65**, 026139 (2002).
[21] M. Barahona and L. M. Pecora, Phys. Rev. Lett. **89**, 054101 (2002).
[22] X. F. Wang and G. Chen, Int. J. Bifurcation Chaos **12**, 187 (2002).
[23] R. K. Esfahani, F. Shahbazi, and K. A. Samani, Phys. Rev. E **86**, 036204 (2012).
[24] D. J. Watts and S. H. Strogatz, Nature (London) **393**, 440 (1998).
[25] H. Daido, Phys. Rev. Lett. **68**, 1073 (1992).

[26] H. Daido, Phys. Rev. E **61**, 2145 (2000).
[27] J. C. Stiller and G. Radons, Phys. Rev. E **58**, 1789 (1998).
[28] J. Gómez-Gardenes, Y. Moreno, and A. Arenas, Phys. Rev. Lett. **98**, 034101 (2007).
[29] T. Nishikawa and A. E. Motter, Phys. Rev. Lett. **117**, 114101 (2016).
[30] Y. Zhang, T. Nishikawa, and A. E. Motter, Phys. Rev. E **95**, 062215 (2017).
[31] Y. Zhang and A. E. Motter, Nonlinearity **31**, R1 (2018).
[32] A. E. Motter and M. Timme, Annu. Rev. Condens. Matter Phys. **9**, 463 (2018).